Eur Biophys J (2006) 36:23–34
DOI 10.1007/s00249-006-0085-3

ARTICLE

Block by internal Mg^{2+} causes voltage-dependent inactivation of Kv1.5

Thomas W. Claydon · Daniel C. H. Kwan · David Fedida · Steven J. Kehl

Received: 6 January 2006 / Revised: 15 June 2006 / Accepted: 26 June 2006 / Published online: 11 August 2006

Abstract Internal Mg^{2+} blocks many potassium channels including Kv1.5. Here, we show that internal Mg^{2+} block of Kv1.5 induces voltage-dependent current decay at strongly depolarised potentials that contains a component due to acceleration of C-type inactivation after pore block. The voltage-dependent current decay was fitted to a bi-exponential function (τ_{fast} and τ_{slow}). Without Mg^{2+}, τ_{fast} and τ_{slow} were voltage-independent, but with 10 mM Mg^{2+}, τ_{fast} decreased from 156 ms at +40 mV to 5 ms at +140 mV and τ_{slow} decreased from 2.3 s to 206 ms. With Mg^{2+}, tail currents after short pulses that allowed only the fast phase of decay showed a rising phase that reflected voltage-dependent unbinding. This suggested that the fast phase of voltage-dependent current decay was due to Mg^{2+} pore block. In contrast, tail currents after longer pulses that allowed the slow phase of decay were reduced to almost zero suggesting that the slow phase was due to channel inactivation. Consistent with this, the mutation R487V (equivalent to T449V in *Shaker*) or increasing external K^+, both of which reduce C-type inactivation, prevented the slow phase of decay. These results are consistent with voltage-dependent open-channel block of Kv1.5 by internal Mg^{2+} that subsequently induces C-type inactivation by restricting K^+ filling of the selectivity filter from the internal solution.

Thomas W. Claydon and Daniel C. H. Kwan contributed equally to the manuscript.

T. W. Claydon · D. C. H. Kwan · D. Fedida · S. J. Kehl (✉)
Department of Cellular and Physiological Sciences,
University of British Columbia, 2350 Health Sciences Mall,
Vancouver, BC, Canada V6T 1Z3
e-mail: skehl@interchange.ubc.ca

Keywords K^+ channel · Mg^{2+} · Inactivation

Introduction

Internal Mg^{2+} is a well-characterised blocker of K^+ channels. Outward movement of K^+ in inward rectifier channels is impeded by internal Mg^{2+} (Horie et al. 1987; Matsuda et al. 1987; Vandenberg 1987), but a number of voltage-gated channels are also sensitive to internal Mg^{2+}. Outward currents through the *Shaker* channel (Harris and Isacoff 1996) as well as members of the mammalian Kv1 family, such as Kv1.1, Kv1.2, Kv1.4, Kv1.5 and Kv1.6 (Ludewig et al. 1993; Gomez-Hernandez et al. 1997; Tammaro et al. 2005), are inhibited by internal Mg^{2+}. Both Kv3 and Kv2.1 channels show inward rectification properties in the presence of internal Mg^{2+} (Rettig et al. 1992; Lopatin and Nichols 1994) and some K^+ channels are also sensitive to external Mg^{2+}, albeit to a much smaller degree (Biermans et al. 1987; Elinder et al. 1998). In all these cases, reduction of current flow is thought to reflect direct pore blockade and/or charge screening by Mg^{2+}, but in none of these instances has promotion of C-type inactivation been suggested as a mechanism of enhanced current decay.

Internal Mg^{2+} binding is voltage-dependent and induces a rapid, open-channel flickery block (Horie et al. 1987; Matsuda et al. 1987) that is relieved by external K^+, which competes with Mg^{2+} at its site of block (Horie et al. 1987; Matsuda 1991). Other internal divalent cations, such as Ca^{2+} and Sr^{2+} (Armstrong and Palti 1991) as well as Ba^{2+} (Armstrong and Taylor 1980; Eaton and Brodwick 1980), cause voltage-dependent block of K^+ current. A number of other

studies have suggested that some large organic cations applied intracellularly can also cause a flickery open channel block of K^+ channels (e.g. quinidine (Fedida 1997)). However, in these cases, the mechanism of block by the cations is proposed to be more complex. The N-terminal domain of some K^+ channels (Choi et al. 1991; Demo and Yellen 1991; Hoshi et al. 1991) and quaternary ammonium (QA) ions are thought to impede K^+ conduction by entering the inner vestibule of the open channel pore, perhaps as deeply as the internal entrance to the selectivity filter (Choi et al. 1991; del Camino et al. 2000; Thompson and Begenisich 2001, 2003; Zhou et al. 2001). Binding of the N-terminal domain or an internal QA ion within the internal pore not only directly impedes K^+ flux but, as a consequence, also greatly enhances C-type inactivation (Baukrowitz and Yellen 1996b). Some QA ions also act allosterically to enhance C-type inactivation (Baukrowitz and Yellen 1996a), as does quinidine (Wang et al. 2003).

C-type inactivation involves a highly cooperative or concerted constriction of the outer mouth of the pore and is sensitive to mutation of residues within the outer pore mouth as well as the presence of K^+ within the pore such that if K^+ is absent the rate of C-type inactivation is enhanced (Lopez-Barneo et al. 1993; Yellen et al. 1994; Ogielska et al. 1995). We use the term C-type inactivation here as a simplified term to describe the complex process of slow inactivation, which is thought to be due to a collapse of the pore (P-type inactivation; De Biasi et al. 1993) followed by stabilisation of the voltage sensor in the outward position resulting in charge immobilisation (C-type inactivation; Chen et al. 1997; Olcese et al. 1997; Loots and Isacoff 2000). Channel block, N-type inactivation, and C-type inactivation can be coupled processes because the onset of these blocking processes accelerates the rate of C-type inactivation (Baukrowitz and Yellen 1995; Rasmusson et al. 1995). This is thought to arise because binding of drugs or the N-terminal inactivation domain within the internal pore restricts the K^+ flux from the internal solution to the selectivity filter and, by decreasing the occupancy of a K^+ binding site near the outer pore mouth, promotes constriction of the pore (Baukrowitz and Yellen 1995).

In the present study, we have asked whether any aspect of the inhibition of Kv1.5 channels at depolarised potentials by internal Mg^{2+} could be attributable to the acceleration of C-type inactivation once the pore was blocked. The presence of internal Mg^{2+} was associated with a voltage-dependent decay of current that could be fitted with two exponential phases. The fast phase was attributed to rapid Mg^{2+} block of the channel, whilst the slower phase represented enhanced, indirectly voltage-dependent C-type inactivation. We propose a mechanism in which occlusion of the open channel by internal Mg^{2+} block restricts K^+ occupancy of the selectivity filter from the internal side of the membrane, and promotes C-type inactivation.

Materials and methods

Molecular biology and cell preparation

Experiments were performed using wild-type or mutant human Kv1.5 channels inserted into the pcDNA3 vector. The R487V point mutation was generated using the Quikchange™ site-directed PCR mutagenesis kit (Stratagene, La Jolla, CA, USA). Stable transfections of HEK293 or mouse *ltk*-cells with wild-type or R487V cDNA and a selection marker for antibiotic resistant growth in G418 sulphate were made using Lipofectamine 2000 reagent (Invitrogen, Carlsbad, CA, USA) in a 1:3 (cDNA:Lipofectamine) ratio. Cells were cultured in MEM nutrient mixture supplemented with 10% foetal bovine serum, 10,000 units/ml penicillin G, 10,000 μg/ml streptomycin sulphate, 25 μg/ml amphotericin B and 0.5 mg/ml G418 sulphate at 37°C in 95% air and 5% CO_2. G418 sulphate (Invitrogen; 0.5 mg/ml) was added 48 h after transfection. Approximately 1×10^5 cells were seeded onto glass cover slips 24 h prior to experiments. All cell culture reagents were obtained from Invitrogen (Mississauga, ON, Canada).

Electrophysiology

Currents were recorded using whole-cell, outside-out or inside-out patch clamp configurations. In all cases, microelectrodes with a resistance of 1.5–3 MΩ were used. Pipette filling solutions varied according to each experiment. For whole-cell and outside-out patch recordings, the pipette contained (mM): 130 KCl, ten HEPES, ten EGTA and 0, 0.1, 0.3, 1, 3 or 10 free $MgCl_2$ titrated to pH 7.4 using KOH. Free Mg^{2+} concentrations were calculated using MaxChelator 2004 (obtained at http://www.stanford.edu/~cpatton/maxc.html). For inside-out patch recordings, the pipette contained (mM): 143.5 NaCl, ten HEPES, two $CaCl_2$, one $MgCl_2$, and five glucose (titrated to pH 7.4 using NaOH). This solution was also used as bath solutions for whole-cell and outside-out patch recordings. For inside-out patch recordings, the bath solution contained 170 KCl, ten HEPES and 0, 0.1, 0.3, 1, 3 or 10 free $MgCl_2$ (titrated to pH 7.4 using KOH). Membrane

currents were recorded using an Axopatch 200A amplifier (Axon Instruments, Union City, CA, USA) with computer driven protocols (pClamp8 software and Digidata 1200B interface, Axon Instruments) or with an EPC-7 patch-clamp amplifier and Pulse + PulseFit software (HEKA Electronik, Lambrecht, Germany). Currents were sampled at 10 kHz and filtered at 2–3 kHz. Whenever possible, leak subtraction was performed using a -P/4 protocol from a holding potential of –80 mV. It was not practical to use leak subtraction with protocols involving pulses longer than 400 ms. Experiments were performed at 20–25°C. Mean ± SEM and n values are shown.

Results

Internal Mg^{2+} causes voltage-dependent decay of Kv1.5 current

Figure 1 shows whole-cell Kv1.5 currents recorded during 400 ms voltage clamp pulses from –80 to +200 mV from a holding potential of –80 mV with internal Mg^{2+} concentrations ranging from 0 to 10 mM. At strongly depolarised potentials, internal Mg^{2+} caused a reduction in peak current and a prominent decay of current that could be fitted to a double exponential function (τ_{fast} and τ_{slow}). To show the fast phase of decay and the effect of Mg^{2+} on the peak current more clearly, the insets in Fig. 1 shows the current during the first 20 ms of each pulse. Figure 2a, b shows mean data for the effect of Mg^{2+} on the voltage-dependence of Kv1.5 current decay. Currents were recorded during 400 ms or 5 s pulses to obtain good fits of τ_{fast} and τ_{slow}. In the absence of Mg^{2+}, both phases of decay were voltage-independent: at +40 and +140 mV, τ_{fast} was 244 ± 32 and 206 ± 48 ms, respectively, and the corresponding values for τ_{slow} were 2.6 ± 0.2 and 3.3 ± 0.9 s (Fig. 2a, b; n = 3–7; not significant (NS), ANOVA). It was not possible to apply pulses long enough (>400 ms) to obtain reliable fits at potentials greater than +140 mV. In contrast, in the presence of 10 mM Mg^{2+}, both phases showed clear voltage-dependence: τ_{fast} was 156 ± 16 and 5.4 ± 1.1 ms and τ_{slow} was 2.3 ± 0.4 s and 206 ± 11 ms at +40 mV and +140 mV, respectively (Fig. 2a, b; n = 6; P < 0.001, ANOVA). Because of the faster decay, it was possible to obtain good fits for τ_{fast} and τ_{slow} up to +200 mV from 400 ms pulses; at +200 mV with 10 mM Mg^{2+}, τ_{fast} was 1.1 ± 0.1 ms and τ_{slow} was 61 ± 31 ms (n = 3). The enhancement of the decay rate was correlated with an increase in the amplitudes of each phase. Without Mg^{2+}, the contributions of the current decay due to both the fast (a_{fast}) and slow (a_{slow}) components were voltage-independent; at +40 and +140 mV a_{fast} was 0.36 ± 0.03 and 0.35 ± 0.07, respectively (n = 6; NS,

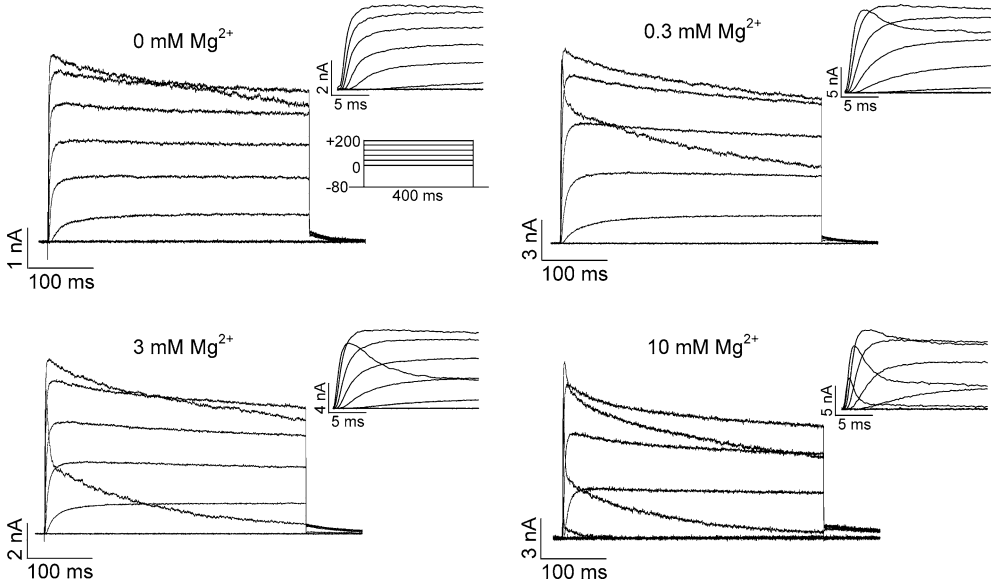

Fig. 1 Mg^{2+} causes voltage-dependent decay of Kv1.5 current. Typical leak-subtracted whole-cell current traces recorded during 400 ms voltage clamp pulses from 0 to +200 mV in 40 mV increments (holding potential = –80 mV) with the indicated internal Mg^{2+} concentration. Insets show the same currents on an expanded time scale to show the effect of Mg^{2+} on the fast phase of decay and on peak current. Each set of records is from a different cell. The decay of current at extreme depolarisation in the absence of internal Mg^{2+} may be due to the presence of the pH buffer HEPES (Guo and Lu 2002). In this and subsequent figures, the voltage protocol used to record currents is shown as an inset

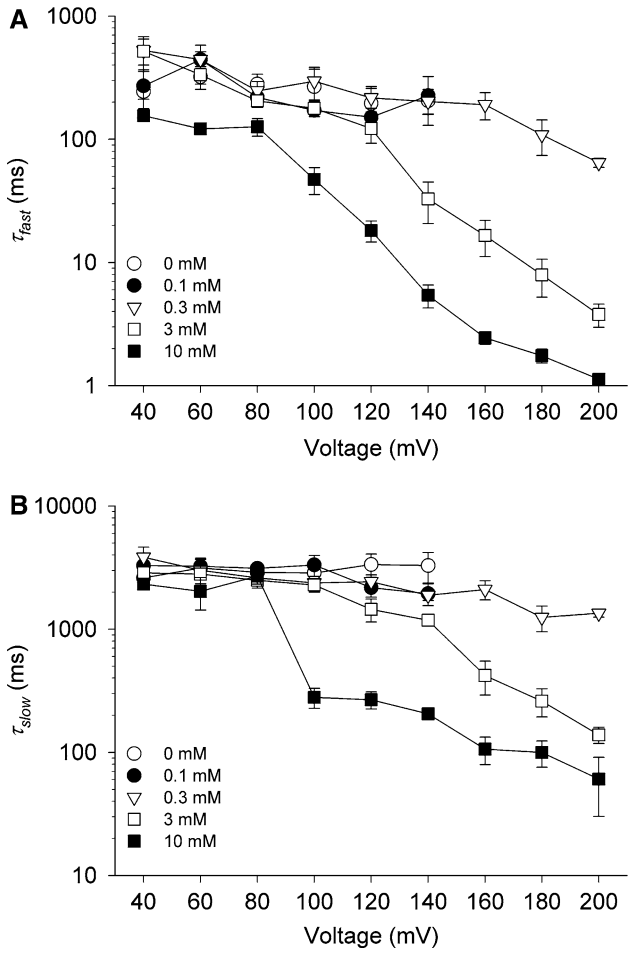

Fig. 2 Mg^{2+}-induced current decay is biexponential. **a** and **b** mean time constants for the fast (**a**, τ_{fast}) and slow (**b**, τ_{slow}) phases of current decay with different internal Mg^{2+} concentrations plotted against membrane potential recorded in the whole-cell configuration such as in Fig. 1 (n = 3–11). To optimise curve fitting to the two components, currents were recorded during either 400 ms or 5 s pulses

ANOVA), and the corresponding values for a_{slow} were 0.09 ± 0.02 and 0.09 ± 0.02 (n = 6; NS, ANOVA). In contrast, with 10 mM Mg^{2+} a_{fast} increased from 0.37 ± 0.03 to 0.56 ± 0.05 (n = 6; P < 0.01, ANOVA) and a_{slow} increased from 0.13 ± 0.01 at +40 mV to 0.26 ± 0.03 at +140 mV (n = 3–7; P < 0.001, ANOVA). These data show that whilst inactivation is largely voltage-independent in the absence of Mg^{2+}, the presence of Mg^{2+} confers a marked voltage-dependence to the current decay. We therefore performed experiments to understand the basis for the two components of current decay.

The fast phase of current decay

Recently, Tammaro et al. (2005) showed that internal Mg^{2+} inhibits Kv1.5 channels. These authors showed that internal Mg^{2+} shifted the voltage-dependence of activation as a result of a charge screening effect, but also reduced current amplitude at potentials at which the open probability was maximal (0 to +70 mV). This suggests that Mg^{2+} may directly block the channel. We therefore reasoned that the fast phase of current decay shown in Fig. 1 at strongly depolarised potentials might represent voltage-dependent block of the pore by internal Mg^{2+}. To test this, we measured tail current characteristics following depolarising pulses of different duration. Figure 3 shows typical whole-cell current traces recorded during 5, 10, 50, 100 and 200 ms pulses from –80 to +180 mV (holding potential –80 mV) in the absence and presence of 10 mM Mg^{2+}. Tail currents at –50 mV following pulses to +100 and +180 mV are expanded in the insets to show channel deactivation. In the absence of Mg^{2+}, tail currents following pulses to +100 and +180 mV were indistinguishable from one another regardless of the pulse duration. In contrast, the presence of internal Mg^{2+} significantly altered tail current characteristics. Tail currents following a 5 ms pulse to +180 mV, which allowed the fast, but not the slow, phase of current decay to occur, were similar to those following a 5 ms pulse to +100 mV except for a prominent rising phase. Since current decay was prominent during a pulse to +180 mV, but was minimal at +100 mV, this suggests that the rising phase of tail currents represents ''unblock'' and that Mg^{2+} block accounts for the fast phase of decay. As the pulse duration was increased to allow the slow phase of current decay to develop, tail currents following a +180 mV pulse were reduced and were almost absent following a 200 ms pulse. This is shown more clearly by the data in Fig. 4a, which shows normalised tail current amplitudes following pulses of different duration to a range of potentials in the absence and presence of Mg^{2+}. Without Mg^{2+}, tail current amplitude was not very sensitive to pulse duration and was only slightly reduced following 400 ms pulses to strongly depolarised potentials (i.e. +160 and +180 mV). However, with 10 mM Mg^{2+}, the peak of the tail current was very sensitive to pulse duration; following a 400 ms pulse to +180 mV, tail current amplitude was reduced to 26 ± 6 % of the value following a pre-pulse to +40 mV (n = 6). This suggests that with 10 mM Mg^{2+}, the majority of channels entered the inactivated state during the pulse and did not recover from inactivation prior to deactivating (see below). In contrast, the peak of the tail current following a 10 ms pulse to +180 mV was largely unchanged (the peak of the tail current following a 400 ms pulse to +180 mV was 90 ± 2% of the value at +40 mV; n = 5).

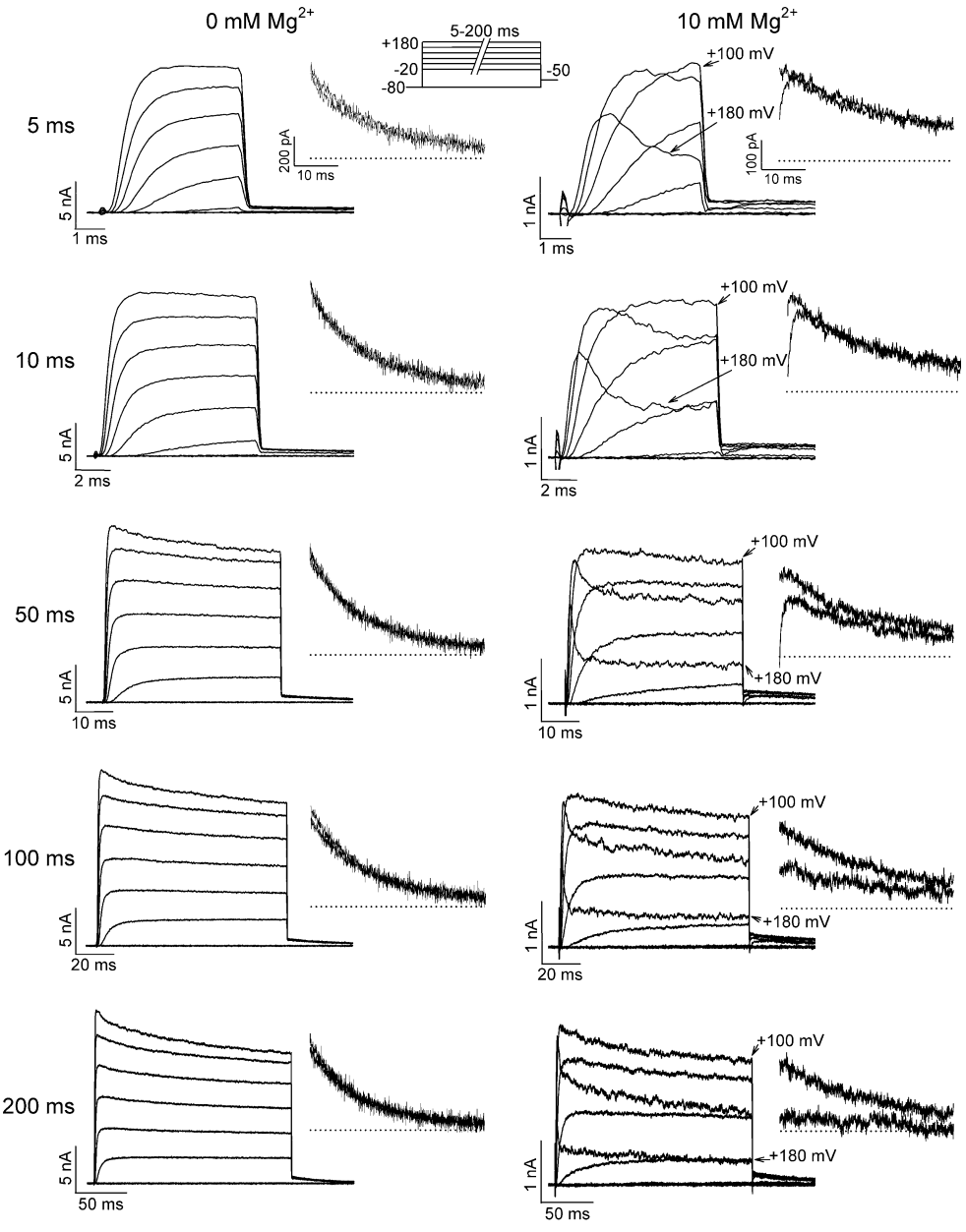

Fig. 3 Tail current kinetics reveal properties of the Mg^{2+}-induced current decay. Typical current traces recorded in the absence and presence of 10 mM Mg^{2+} during 5, 10, 50, 100 or 200 ms voltage clamp pulses from –20 to +180 mV in 40 mV increments (holding potential = –80 mV). Insets show tail currents following pulses to +100 and +180 mV with expanded time and current scales. In this and subsequent figures, the *dotted line* denotes the zero current level

Comparison of tail currents following a 5 ms pulse to +180 mV in the absence and presence of Mg^{2+} (Fig. 4b) shows further evidence that Mg^{2+} is an open channel blocker of the Kv1.5 pore. In the presence of Mg^{2+}, tail currents showed a prominent rising phase and a slower decay, which are features that reflect a rapid unblock prior to channel closure and a slower time course of closing. Figure 4c shows the time constant of deactivation in the absence and presence of Mg^{2+}. Ten millimolar Mg^{2+} slowed the time constant of channel closing approximately twofold from 19 ± 2 to 42 ± 7 ms (n = 5–8; $P < 0.01$, t-test).

Raising the external K^+ concentration relieves internal Mg^{2+} block of potassium channels by competing with the blocking ion (Horie et al. 1987; Matsuda 1991; Harris and Isacoff 1996). Figure 5a shows typical currents recorded from the same cell during a 15 ms pulse to +180 mV (following a 10 ms pulse to +50 mV to open the channels) in the presence of 10 mM internal Mg^{2+} and the indicated external concentration of K^+. Increasing the concentration of external K^+ slowed and reduced the extent of the fast phase of decay in the presence of internal Mg^{2+}. This is shown more clearly in Fig. 5b, c, which show, respectively, mean data for the time constant and fractional amplitude of the fast phase of decay over a range of potentials. The values for τ_{fast} differ from those reported in Fig. 2a because here they were measured

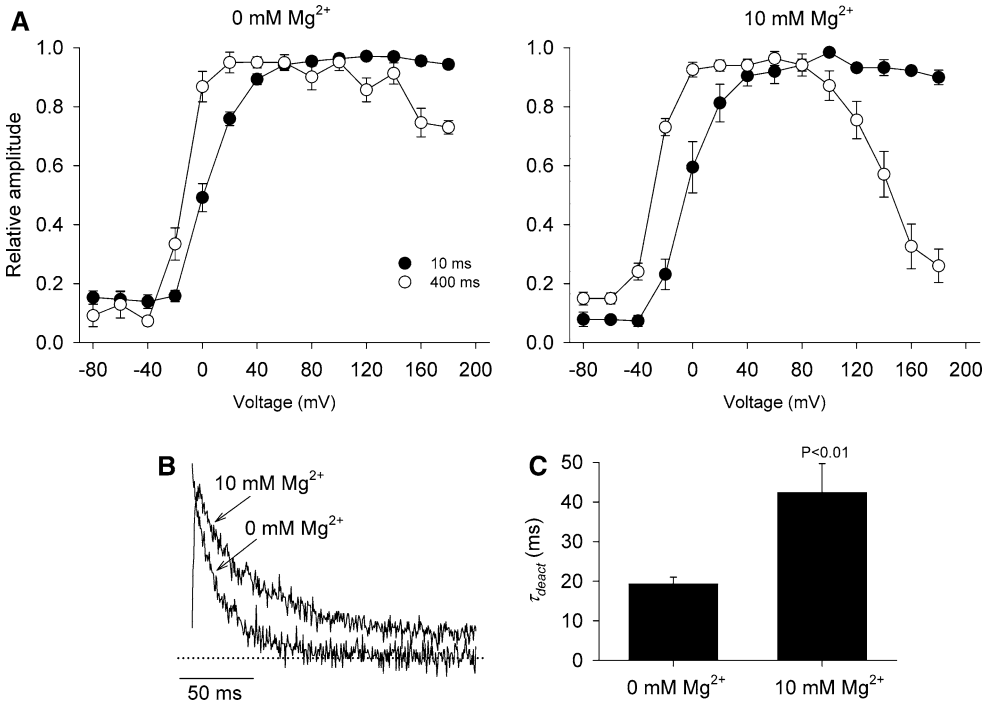

Fig. 4 The fast phase of current decay is due to Mg^{2+} block of the open pore. **a** mean normalised tail current amplitudes following pulses of different duration plotted against the membrane potential in the absence and presence of 10 mM Mg^{2+}. Peak tail current amplitudes are normalised to the maximal peak tail current, **b** typical tail currents recorded in the absence and presence of 10 mM Mg^{2+} following a 5 ms pulse to +180 mV showing the prominent rising phase and slowed closure in the presence of Mg^{2+} and **c** mean time constants of deactivation in the absence and presence of 10 mM Mg^{2+} measured from currents such as those shown in **b**

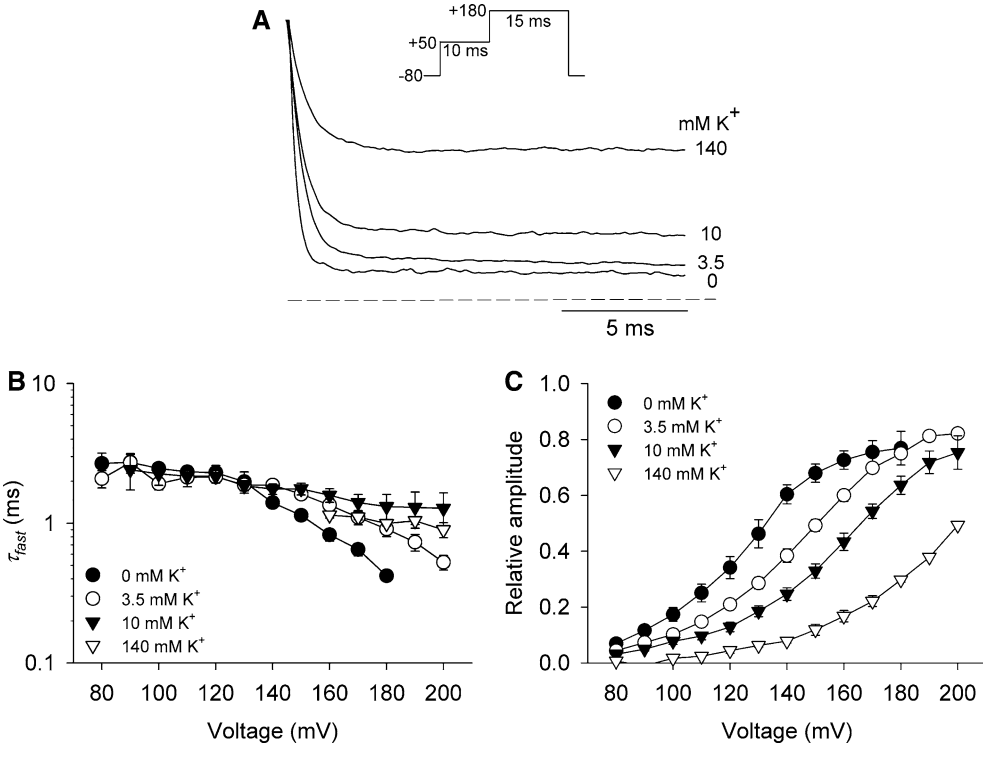

Fig. 5 Raising the external K^+ concentration relieves internal Mg^{2+} block. **a** Typical current traces recorded from the same cell during a 15 ms pulse to +180 mV (following a 10 ms pulse to +50 mV to open the channels; not shown) in the presence of 10 mM internal Mg^{2+} and the indicated external concentration of K^+. Each current trace is normalised with respect to its peak, **b** and **c** mean time constants (**b**) and fractional amplitudes (**c**) for the fast phase of decay over a range of potentials with different external K^+ concentrations (n = 3–9)

following a pre-pulse to +50 mV that allowed channel opening prior to stepping to the test potential. This was not the case in Fig. 2a where the Mg^{2+} blocking time course appears slower because channels must open before block can proceed. The rightward shift of the fractional amplitude curve with increasing external K^+ (Fig. 5c) suggests that there is an antagonistic interaction between K^+ and Mg^{2+}. Although the slow phase was also sensitive to the external K^+ concentration (see below), it is unlikely to contribute significantly in these experiments given the brevity (15 ms) of the voltage pulse. Taken together, the observations in Figs. 3, 4

and 5 strongly suggest that the fast phase of current decay is due to voltage-dependent block of open channels by internal Mg^{2+}.

Since the current traces shown in Fig. 1 probably reflect channels that are rapidly blocked upon opening, calculation of the binding affinity from the reduction of peak current amplitude is precluded. Therefore, we performed another set of experiments to investigate the characteristics of Mg^{2+} block. Figure 6a shows typical current traces recorded from the same inside-out patch using 0.1 or 10 mM internal Mg^{2+} during 10 ms pulses to +40 mV immediately followed by 15 ms test pulses from –40 to +200 mV. By using a 10 ms pre-pulse to +40 mV, we could measure Mg^{2+} block of open channels without interference from channel activation. Current at the end of the 15 ms test pulse was used to construct the current–voltage relationships shown in Fig. 6b. Data points were fitted with the equation:

$$I(V,[Mg^{2+}]) = (0.20 + 0.00395V)/(1 + [Mg^{2+}]/(K_D(0\,\mathrm{mV})\exp(-z\delta FV/RT))), \quad (1)$$

where V is the membrane voltage, z the valence (i.e. 2), K_D (0 mV) the dissociation constant for Mg^{2+} at 0 mV, δ the fractional electrical distance of the Mg^{2+} binding site, and F, R and T have their usual meaning. K_D (0 mV) and δ values were 1.5 ± 0.5 M and 0.47 ± 0.02, respectively, at 1 mM Mg^{2+} and the corresponding values at 10 mM Mg^{2+} were 0.8 ± 0.3 M and 0.45 ± 0.04 (n = 3–4).

Recovery from inactivation

Since Mg^{2+} had profound effects on the decay of Kv1.5 current, it was important to understand the effects of internal Mg^{2+} on the recovery from inactivation. Figure 7a shows typical current traces recorded in the absence and presence of 10 mM Mg^{2+} during a modified protocol to measure the time course of recovery of Kv1.5 channels from inactivation. Due to patch instability at extreme depolarisations, currents were recorded during an initial 20 ms test pulse to +40 mV (marked by the arrow) followed by a conditioning pulse and then 20 ms test pulses to +40 mV following different intervals at –80 mV. In an attempt to standardise the proportion of channels entering the inactivated state, the conditioning pulse was a 5 s voltage step to +60 mV in the absence of Mg^{2+} and a 600 ms voltage step to +180 mV in the presence of 10 mM Mg^{2+}. This approach was only partly successful due to the rapid decay of current with 10 mM Mg^{2+}. Figure 7b shows the mean time course of recovery of Kv1.5 channels from inactivation in the absence and presence of 10 mM Mg^{2+}. In both cases, recovery was fitted to a double exponential function (τ_1 and τ_2). With 10 mM Mg^{2+} there was no effect on either the time constant or

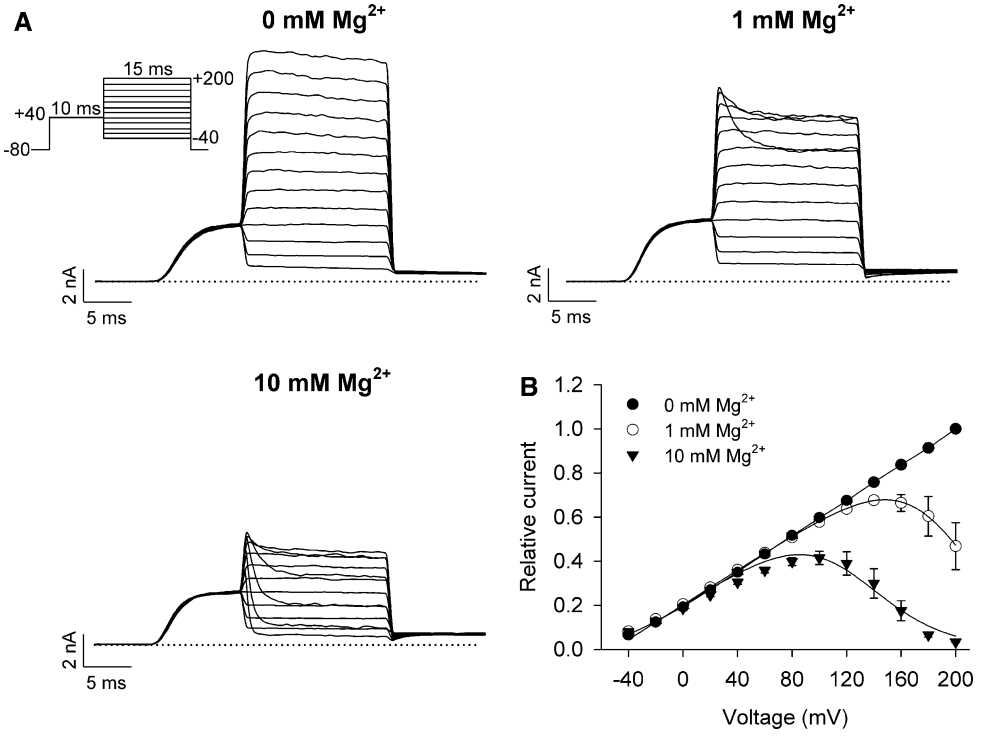

Fig. 6 Mg^{2+} sensitivity of wild-type Kv1.5. **a** Currents recorded from the same inside-out patch with 0, 1 or 10 mM internal Mg^{2+} during a 10 ms voltage pulse to +40 mV followed immediately by 15 ms pulses from –40 to +200 mV, **b** mean current at the end of the 15 ms pulse normalised to the peak current at +200 mV in the absence of Mg^{2+} and plotted against membrane potential with a range of internal Mg^{2+} concentrations. Data were fitted with (1). The K_D (0 mV) and δ values for 1 mM Mg^{2+} were 1.5 ± 0.5 M and 0.47 ± 0.02, respectively, and the equivalent values for 10 mM Mg^{2+} were 0.8 ± 0.3 M and 0.45 ± 0.04 (n = 3–4)

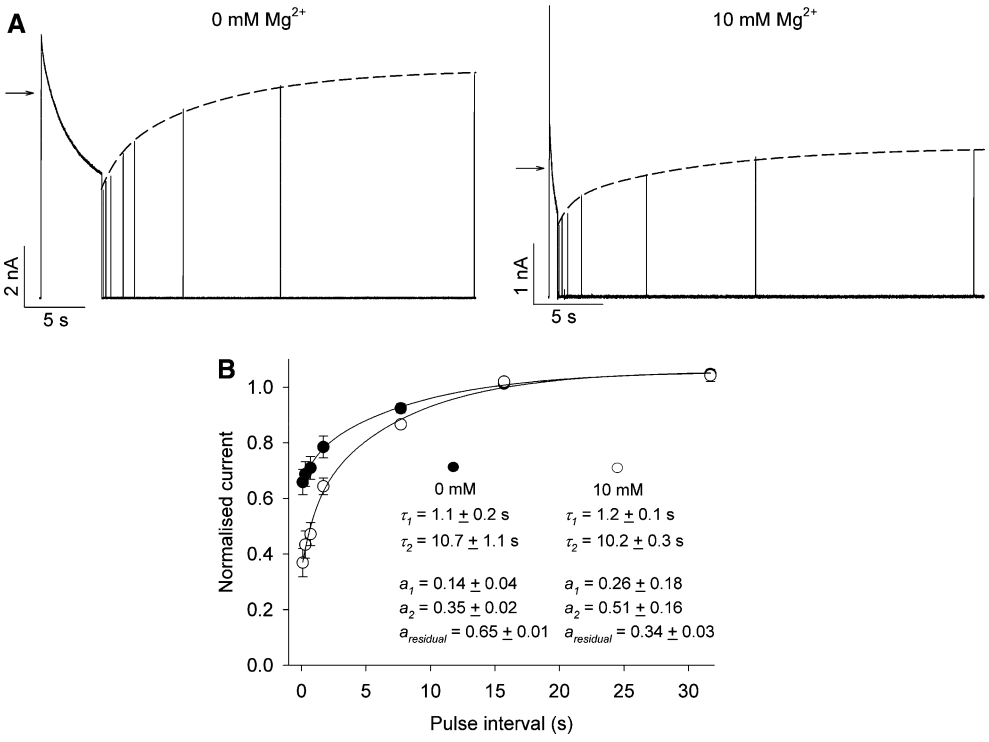

Fig. 7 Internal Mg^{2+} has no effect on recovery from inactivation. **a** Typical traces recorded in the whole-cell configuration with 0 or 10 mM internal Mg^{2+} during a modified recovery from inactivation protocol. Currents were recorded during a 20 ms pre-pulse to +40 mV that was followed immediately by a conditioning pulse to +60 mV for 5 s (with 0 mM Mg^{2+}) or to +180 mV for 600 ms (with 10 mM Mg^{2+}) and then 20 ms test pulses to +40 mV following intervals of 0.1, 0.32, 0.74, 1.76, 3.8, 8.7, 16.9 and 33.1 s at –80 mV. It was assumed that each test pulse did not induce further inactivation. *Dashed lines* show a bi-exponential fit of the data. *Arrows* mark current amplitude during the +40 mV prepulse, **b** mean time course of the recovery from inactivation in the absence and presence of Mg^{2+}. *Solid lines* describe fits of the data using two exponential functions with time constants, τ_1 and τ_2. The inset shows the values for τ_1 and τ_2 with and without Mg^{2+} ($n = 4$)

contribution of either phase of recovery from inactivation: in the absence and presence of 10 mM Mg^{2+}, τ_1 was 1.1 ± 0.2 and 1.2 ± 0.1 s, respectively, and the corresponding values for τ_2 were 10.7 ± 1.1 and 10.2 ± 0.3 s ($n = 5$; NS, *t*-test). These data suggest that the time course of recovery in the presence of Mg^{2+} reflects the transition of channels from the same inactivated states as in the absence of Mg^{2+} rather than a slow recovery from Mg^{2+} block.

The slow phase of current decay

The experiments in Figs. 3, 4 and 5 suggest that the fast phase of decay in the presence of internal Mg^{2+} represents fast open channel block of the pore. Tammaro et al. (2005) suggested that Mg^{2+} block might induce inactivation of Kv1.5. In order to test this and to understand the mechanistic basis of the slow phase of decay, we investigated the effect of internal Mg^{2+} on the slow phase using manipulations known to affect C-type inactivation. Figure 8a shows typical current traces recorded from mutant Kv1.5 channels in which the R487 residue at the outer mouth of the pore was replaced with a valine residue (R487V). Mutation of the equivalent residue in the *Shaker* channel has been shown to abolish C-type inactivation (Lopez-Barneo et al. 1993) and the R487V mutation in Kv1.5 dramatically inhibits inactivation of Na^+ current (Wang et al. 2000). Na^+ permeation of the channel (Fedida et al. 1999). Currents were recorded in the absence and presence of 10 mM Mg^{2+} during 400 ms voltage pulses from –80 to +200 mV. The R487V mutation reduced the effect of 10 mM Mg^{2+} to such an extent that it was not possible to obtain reliable fits of the slow phase of current decay during 400 ms pulses. Figure 8b shows, on an expanded scale, the pulse current decay after fast block by 10 mM Mg^{2+} had reduced current by approximately 90% (percentage current reduction was measured in relation to the maximal observed current, therefore, this may be an underestimate due to block by Mg^{2+} at lower potentials). Following Mg^{2+} block, inactivation is enhanced in the wild-type channel, as shown above, but this is abolished in the R487V mutant channel

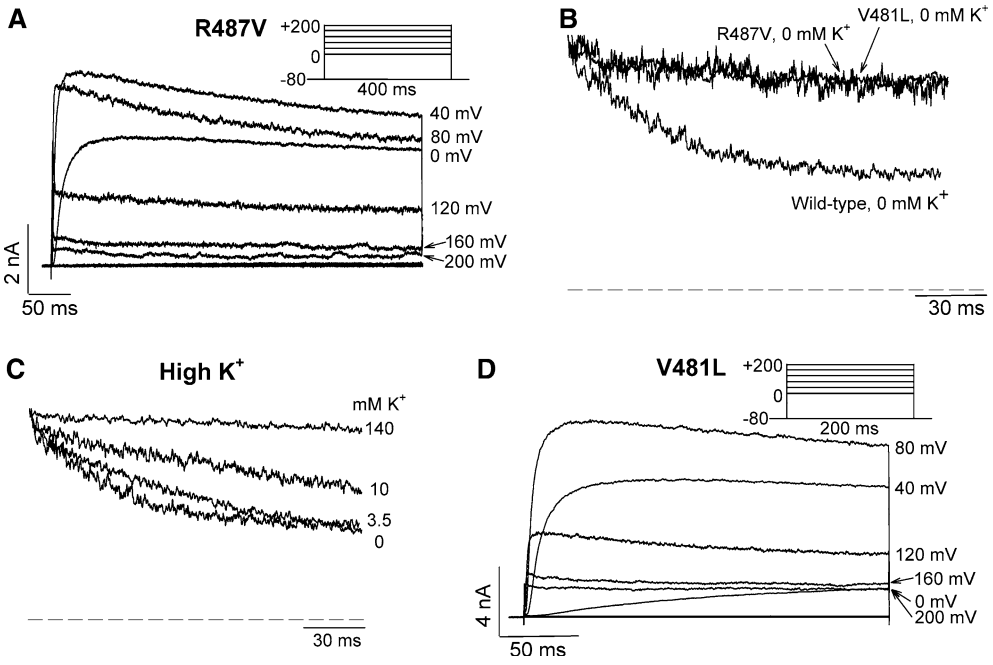

Fig. 8 The slow phase of current decay following Mg^{2+} block is due to enhanced C-type inactivation. **a** Typical current traces recorded from R487V mutant channels in the presence of 10 mM Mg^{2+} during 400 ms voltage clamp pulses (as in Fig. 1) from 0 to +200 mV in 40 mV increments (holding potential = –80 mV), **b** typical currents recorded from wild-type, R487V and V481L mutant channels showing inactivating current following approximately 90% block by Mg^{2+} and **c** typical currents recorded from wild-type channels in the presence of the indicated external K^+ concentration showing inactivating current following approximately 90% block by Mg^{2+}. *Block* was significantly less with 140 mM K^+ (see text) and **d** typical current traces recorded from V481L mutant channels in the presence of 10 mM Mg^{2+} during 200 ms voltage clamp pulses from –80 to +200 mV in 40 mV increments (holding potential = –80 mV). For each panel, similar recordings were obtained from 4 to 8 other cells

(Fig. 8b). Interestingly, the R487V mutation enhanced Mg^{2+} binding. With 10 mM Mg^{2+}, K_D (0 mV) and δ values for the mutant channel were 19 ± 1 mM and 0.35 ± 0.01, respectively, compared with 830 ± 350 mM and 0.45 ± 0.04, respectively, for the wild-type channel. Figure 8c shows that inhibition of C-type inactivation by raising the external K^+ concentration (Lopez-Barneo et al. 1993) also abolished the enhancement of inactivation following approximately 90% block by 10 mM Mg^{2+}. Since the extent of Mg^{2+} block was sensitive to the external K^+ concentration (Fig. 5), inactivation in Fig. 8c was measured during pulses to +180 mV. Figure 5c shows that the effect of external K^+ (0–10 mM K^+) on the extent of block was minimal at this potential. Data with 140 mM K^+ are shown for reference only since they represent inactivation following significantly less block than with other K^+ concentrations (Fig. 5c). These data show that the enhanced slow phase of decay following Mg^{2+} block represents enhanced C-type inactivation.

Baukrowitz and Yellen (1996b) previously showed that block of the *Shaker* channel by internal TEA^+ derivatives enhanced inactivation by impeding internal K^+ access to the selectivity filter thereby indirectly promoting collapse of the outer pore. Additionally, the ability of the blocking ion to induce inactivation was shown to be dependent on its dwell time (Baukrowitz and Yellen 1996b). Figure 8d shows typical current traces recorded from mutant Kv1.5 channels in which the residue V481 at the base of the selectivity filter was replaced with a leucine residue (V481L). Mutation of the equivalent residue in the Kv3.1 channel has been shown to significantly reduce the dwell time of Mg^{2+} at its block site (Harris and Isacoff 1996). Currents in Fig. 8d were recorded in the presence of 10 mM Mg^{2+} during 200 ms voltage pulses from –80 to +200 mV. Similar to the effect of the R487V mutation (Fig. 8a), the V481L mutation reduced the effect of Mg^{2+} on the slow phase of current decay. Figure 8b shows the current decay of V481L channels after fast block by 10 mM Mg^{2+} had reduced current by approximately 90%. The V481L mutant channel abolished the Mg^{2+}-induced inactivation without affecting C-type inactivation; in the absence of Mg^{2+}, the time constants of the two phases of inactivation, $\tau_{inact,fast}$ and $\tau_{inact,slow}$, were 413 ± 124 ms and 2.6 ± 0.7 s, respectively compared with corresponding values of 281 ± 46 ms and 2.4 ± 0.3 s in the wild-type channel (n = 6–11; t-test, NS).

Discussion

In the present study, we demonstrate that internal Mg^{2+} causes a voltage-dependent biphasic decay of Kv1.5 current at strongly depolarised potentials. We show that the fast phase of current decay represents voltage-dependent binding of Mg^{2+} within the open channel pore, whilst the slow phase represents C-type inactivation that is induced by Mg^{2+} block of the channel. We explain these data based on a previous model (Baukrowitz and Yellen 1995, 1996b) that suggests that binding of the N-terminal inactivation domain or an internal QA ion enhances C-type inactivation by restricting the flux of internal K^+ to the selectivity filter therefore promoting collapse of the outer pore.

Internal Mg^{2+} rapidly blocks the open Kv1.5 channel

The fast phase of decay was enhanced approximately 150-fold at +200 mV compared to that at +40 mV in 10 mM Mg^{2+} (Fig. 2a, b) and we propose that this reflects voltage dependent Mg^{2+} block of the channel. Consistent with this, tail currents in the presence of Mg^{2+} revealed that channels were not inactivated following short pulses (Fig. 3) and showed a relief from block and slowed channel closure (Figs. 3, 4b, c). The slower deactivation rate (at –50 mV) with Mg^{2+} may represent the balance between Mg^{2+} unbinding and channel closure; alternatively, it may be the result of a charge screening effect due to Mg^{2+} as has been shown to occur in Kv1.5 (Tammaro et al. 2005). These authors showed that the open probability of Kv1.5 channels at –40 mV was significantly higher in the presence than in the absence of 10 mM Mg^{2+}, which is consistent with the slowed channel closure seen in the present study (Fig. 4b). Furthermore, just as Mg^{2+} block of inwardly rectifying channels was relieved by raising external K^+ (Matsuda 1991), increasing extracellular K^+ reduced the effect of Mg^{2+} on the amplitude and decay rate of the fast phase of current decay (Fig. 5). This is consistent with a competitive inhibition of Mg^{2+} block by external K^+. These data strongly suggest that the fast phase of current decay is due to voltage-dependent open channel block of the pore by Mg^{2+}.

Internal Mg^{2+} block induces enhanced C-type inactivation

Following activation, Kv1.5 current decays as channels slowly enter the C-type inactivated state, a process that involves constriction of the outer pore, and which is dependent on evacuation of K^+ from the selectivity filter (Lopez-Barneo et al. 1993; Yellen et al. 1994; Ogielska et al. 1995). In the absence of Mg^{2+}, the slow phase of Kv1.5 current decay was voltage-independent (Fig. 2a, b), as has been reported for *Shaker* channels, but in the presence of 10 mM Mg^{2+} the slow phase was accelerated approximately 40-fold during a strong depolarisation (Fig. 2a, b).

Consistent with the notion that the enhanced slow phase may be due to enhancement of C-type inactivation as the pore is blocked, reduction or abolition of C-type inactivation by either raising the external K^+ concentration or the R487V mutation abolished the voltage-dependent enhancement of the slow phase following Mg^{2+} block (Fig. 8a–c). Raising external K^+ to 140 mM increases the probability of K^+ coordination within the selectivity filter so that collapse of the pore is hindered and therefore C-type inactivation is slowed. Given that when C-type inactivation was abolished, Mg^{2+} block was no longer associated with an enhanced slow phase of decay, these data strongly suggest that the voltage-dependent slow phase of current decay observed following Mg^{2+} block of the channel is due to enhanced C-type inactivation.

Interestingly, the R487V mutation enhanced Mg^{2+} binding. The K_D (0 mV) value for the mutant channel was reduced by ~40-fold. Mutation of the equivalent residue in the Kv1.4 channel (K533Y) caused a ~30-fold decrease in the K_D for Mg^{2+} block (Ludewig et al. 1993). Figure 8a shows that the fast phase of current decay was abolished by the R487V mutation. The abolition of the fast phase of current decay in the R487V mutation (Fig. 8a) is consistent with a faster on rate (k_{on}) for Mg^{2+} block.

Baukrowitz and Yellen (1995, 1996b) described a model in which occlusion of the inner pore, either by the N-terminal inactivation domain or a QA ion, enhanced C-type inactivation by preventing K^+ efflux from the intracellular solution and thereby speeded C-type inactivation. This is consistent with studies that suggest that the inactivation domain and QA ions may enter the open channel as deeply as the base of the selectivity filter (Choi et al. 1991; del Camino et al. 2000; Thompson and Begenisich 2001, 2003; Zhou et al. 2001). We suggest that a similar model describes the enhanced inactivation following internal Mg^{2+} block of the Kv1.5 channel. The mutation equivalent to V481L in the Kv1.5 channel reduces the dwell time of Mg^{2+} at its binding site in the Kv3.1 channel by approximately fourfold at +140 mV (Harris and Isacoff 1996). In a model of QA block of *Shaker* (Baukrowitz and Yellen 1996b), QA ions with shorter dwell times, such as TEA^+, did not induce inactivation because they did not

restrict K^+ flux for long enough to initiate collapse of the pore. The data in Fig. 8b, d shows that this is also the case for Mg^{2+} block of Kv1.5. Since the time constant of Mg^{2+} block is dependent on the off rate, and assuming that k_{on} is unchanged, the abolition of the fast phase of current decay in the V481L mutation (Fig. 8d) is consistent with a reduced Mg^{2+} dwell time within the pore. Figure 8b shows that the reduction of the Mg^{2+} dwell time by the V481L mutation to a value similar to that of TEA^+ in *Shaker* (Harris and Isacoff 1996), also abolished the Mg^{2+}-induced inactivation following block.

The Mg^{2+} binding site

Previous studies suggest that in different types of K^+ channel internal Mg^{2+} binds at a site positioned at an electrical distance (δ) of 0.28–0.54 measured from the inside (Horie et al. 1987; Ludewig et al. 1993; Lopatin and Nichols 1994; Harris and Isacoff 1996). From the data shown in Fig. 6a, we calculated the δ value for Mg^{2+} block of Kv1.5 to be ~0.46 (Fig. 6b). This is similar to previous reports in *Shaker* ($\delta = 0.54$) and Kv1.4 ($\delta = 0.5$) channels and suggests a binding site near to the internal entrance of the selectivity filter. It is clear in Fig. 6b, however, that although the fitted curves (which assume a Hill coefficient of 1) provide a reasonable description of the experimental data, there is some deviation, particularly at 10 mM Mg^{2+}. This alludes to a more complex mechanism of Mg^{2+} block, which may involve more than one blocking site, coupling of Mg^{2+} with the permeant ion, as has been suggested to occur during Cs^+ block of Ca^{2+}-activated K^+ channels (Cecchi et al. 1987), or an allosteric effect on pore structure associated with Mg^{2+} binding similar to that suggested following binding of QA ions to *Shaker* channels (Baukrowitz and Yellen 1996a). The δ value reported by Tammaro et al. (2005) for Mg^{2+} block of Kv1.5 ($\delta = 0.11$) may differ because of complications associated with the presence of Tris buffer present in the internal recording solutions (Tammaro et al. 2005).

It is possible that the measurement of Mg^{2+} block in the present study may be an underestimate due to an unknown contribution to the fast decay of current by the fast component of inactivation since it is known that inactivation of Kv1.5 channels consists of both a fast and slow component. However, we assume this contribution to be small based on two observations: (1) the data in Fig. 3 suggest that little channel inactivation occurs following short pulses that allow only the fast phase of decay as shown by the presence of robust tail currents; (2) if the fast phase contained a significant component due to inactivation, then it should be affected by the cumulative inactivation induced by Mg^{2+} during repetitive pulsing, yet neither the amplitude nor the time constant of decay of the fast phase was affected by the frequency of stimulation (data not shown).

Of particular interest in this study, is the observation that inactivation of Kv1.5 channels becomes voltage-dependent and very rapid as a result of voltage-dependent internal Mg^{2+} block. Unlike other voltage-gated channels, inactivation of hERG (human ether a go–go related gene) channels is very rapid and seems to be intrinsically voltage-dependent (Sanguinetti et al. 1995). The mechanism of the rapid, voltage-dependent inactivation of hERG channels is poorly understood, but it is interesting that Mg^{2+} block confers similar behaviour to Kv1.5.

Acknowledgments We thank Yan Liu and Fifi Ka-Kee Chiu for the preparation of cells. T. W. Claydon is supported by a Post-doctoral Fellowship funded by a Focus on Stroke strategic initiative from The Canadian Stroke Network, the Heart and Stroke Foundation, the CIHR Institute of Circulatory and Respiratory Health and the CIHR/Rx&D Program along with AstraZeneca Canada. D. C. H. Kwan is supported by the Michael Smith Foundation and by a Postgraduate Scholarship from NSERC. Supported by research grants from CIHR and the HSF (DF) and NSERC (SK).

References

Armstrong CM, Palti Y (1991) Potassium channel block by internal calcium and strontium. J Gen Physiol 97:627–638

Armstrong CM, Taylor SR (1980) Interaction of barium ions with potassium channels in squid giant axons. Biophys J 30:473–488

Baukrowitz T, Yellen G (1995) Modulation of K^+ current by frequency and external $[K^+]$: a tale of two inactivation mechanisms. Neuron 15:951–960

Baukrowitz T, Yellen G (1996a) Two functionally distinct subsites for the binding of internal blockers to the pore of voltage-activated K^+ channels. Proc Natl Acad Sci USA 93:13357–13361

Baukrowitz T, Yellen G (1996b) Use-dependent blockers and exit rate of the last ion from the multi-ion pore of a K^+ channel. Science 271:653–656

Biermans G, Vereecke J, Carmeliet E (1987) The mechanism of the inactivation of the inward-rectifying K current during hyperpolarising steps in guinea-pig ventricular myocytes. Pflugers Arch 410:604–613

Cecchi X, Wolff D, Alvarez O, Latorre R (1987) Mechanisms of Cs^+ blockade in a Ca^{2+}-activated K^+ channel from smooth muscle. Biophys J 52:707–716

Chen FSP, Steele D, Fedida D (1997) Allosteric effects of permeating cations on gating currents during K^+ channel deactivation. J Gen Physiol 110:87–100

Choi KL, Aldrich RW, Yellen G (1991) Tetraethylammonium blockade distinguishes two inactivation mechanisms in voltage-activated K^+ channels. Proc Natl Acad Sci USA 88:5092–5095

De Biasi M, Hartmann HA, Drewe JA, Taglialatela M, Brown AM, Kirsch GE (1993) Inactivation determined by a single site in K^+ pores. Pflugers Arch 422:354–363

del Camino D, Holmgren M, Liu Y, Yellen G (2000) Blocker protection in the pore of a voltage-gated K^+ channel and its structural implications. Nature 403:321–325

Demo SD, Yellen G (1991) The inactivation gate of the *Shaker* K^+ channel behaves like an open-channel blocker. Neuron 7:743–753

Eaton DC, Brodwick MS (1980) Effects of barium on the potassium conductance of squid axon. J Gen Physiol 75:727–750

Elinder F, Liu Y, Arhem P (1998) Divalent cation effects on the *Shaker* K^+ channel suggest a pentapeptide sequence as determinant of functional surface charge density. J Membr Biol 165:183–189

Fedida D (1997) Gating charge and ionic currents associated with quinidine block of human Kv1.5 delayed rectifier channels. J Physiol 499:661–675

Gomez-Hernandez JM, Lorra C, Pardo LA, Stuhmer W, Pongs O, Heinemann SH, Elliott AA (1997) Molecular basis for different pore properties of potassium channels from the rat brain Kv1 gene family. Pflugers Arch 434:661–668

Guo D, Lu Z (2002) IRK1 inward rectifier K^+ channels exhibit no intrinsic rectification. J Gen Physiol 120:539–551

Harris RE, Isacoff EY (1996) Hydrophobic mutations alter the movement of Mg^{2+} in the pore of voltage-gated potassium channels. Biophys J 71:209–219

Horie M, Irisawa H, Noma A (1987) Voltage-dependent magnesium block of adenosine-triphosphate-sensitive potassium channel in guinea-pig ventricular cells. J Physiol 387:251–272

Hoshi T, Zagotta WN, Aldrich RW (1991) Two types of inactivation in *Shaker* K^+ channels: effects of alterations in the carboxy-terminal region. Neuron 7:547–556

Loots E, Isacoff EY (2000) Molecular coupling of S4 to a K^+ channel's slow inactivation gate. J Gen Physiol 116:623–636

Lopatin AN, Nichols CG (1994) Internal Na^+ and Mg^{2+} blockade of DRK1 (Kv2.1) potassium channels expressed in *Xenopus* oocytes. Inward rectification of a delayed rectifier. J Gen Physiol 103:203–216

Lopez-Barneo J, Hoshi T, Heinemann SH, Aldrich RW (1993) Effects of external cations and mutations in the pore region on C-type inactivation of *Shaker* potassium channels. Receptors Channels 1:61–71

Ludewig U, Lorra C, Pongs O, Heinemann SH (1993) A site accessible to extracellular TEA^+ and K^+ influences intracellular Mg^{2+} block of cloned potassium channels. Eur Biophys J 22:237–247

Matsuda H (1991) Effects of internal and external Na^+ ions on inwardly rectifying K^+ channels in guinea-pig ventricular cells. J Physiol 460:311–326

Matsuda H, Saigusa A, Irisawa H (1987) Ohmic conductance through the inwardly rectifying K channel and blocking by internal Mg^{2+}. Nature 325:156–159

Ogielska EM, Zagotta WN, Hoshi T, Heinemann SH, Haab J, Aldrich RW (1995) Cooperative subunit interactions in C-type inactivation of K^+ channels. Biophys J 69:2449–2457

Olcese R, Latorre R, Toro L, Bezanilla F, Stefani E (1997) Correlation between charge movement and ionic current during slow inactivation in *Shaker* K^+ channels. J Gen Physiol 110:579–589

Rasmusson RL, Morales MJ, Castellino RC, Zhang Y, Campbell DL, Strauss HC (1995) C-type inactivation controls recovery in a fast inactivating cardiac K^+ channel (Kv1.4) expressed in *Xenopus* oocytes. J Physiol 489:709–721

Rettig J, Wunder F, Stocker M, Lichtinghagen R, Mastiaux F, Beckh S, Kues W, Pedarzani P, Schroter KH, Ruppersberg JP (1992) Characterization of a Shaw-related potassium channel family in rat brain. EMBO J 11:2473–2486

Sanguinetti M, Jiang C, Curran ME, Keating MT (1995) A mechanistic link between an inherited and an acquired cardiac arrhythmia: HERG encodes the I_{Kr} potassium channel. Cell 81:299–307

Tammaro P, Smirnov SV, Moran O (2005) Effects of intracellular magnesium on Kv1.5 and Kv2.1 potassium channels. Eur Biophys J 34:42–51

Thompson J, Begenisich T (2001) Affinity and location of an internal K^+ ion binding site in *Shaker* K channels. J Gen Physiol 117:373–384

Thompson J, Begenisich T (2003) Functional identification of ion binding sites at the internal end of the pore in *Shaker* K^+ channels. J Physiol 549:107–120

Vandenberg CA (1987) Inward rectification of a potassium channel in cardiac ventricular cells depends on internal magnesium ions. Proc Natl Acad Sci USA 84:2560–2564

Wang Z, Hesketh JC, Fedida D (2000) A high Na^+ conductance state during recovery from inactivation in the K^+ channel Kv1.5. Biophys J 79:2416–2433

Wang S, Morales MJ, Qu YJ, Bett GC, Strauss HC, Rasmusson RL (2003) Kv1.4 channel block by quinidine: evidence for a drug-induced allosteric effect. J Physiol 546:387–401

Yellen G, Sodickson D, Chen TY, Jurman ME (1994) An engineered cysteine in the external mouth of a K^+ channel allows inactivation to be modulated by metal binding. Biophys J 66:1068–1075

Zhou M, Morais-Cabral JH, Mann S, MacKinnon R (2001) Potassium channel receptor site for the inactivation gate and quaternary amine inhibitors. Nature 411:657–661